

# Coulomb blockade in Quantum Dots

**Additional reading complementing the lecture notes.<sup>1</sup>**

**Version: 23/04/2007 - Andreas Fuhrer/Carina Fasth**

In the resonant tunnelling diode we have treated electrons as non interacting particles. We have discussed their wave nature, which led to quantized energy states in small and coherent cavities. Qualitatively this is due to the requirement that an integer number of Fermi wavelengths has to fit between the barriers.

Here we begin in the opposite limit by neglecting space quantization effects in terms of self-interference and discussing single electron charging of small metallic islands. Due to the small Fermi-wavelength in metals the energy spectrum of such a system is quasi-continuous and the system can be treated classically, except that due to the quantization of charge an integer number of particles needs to reside on the island.

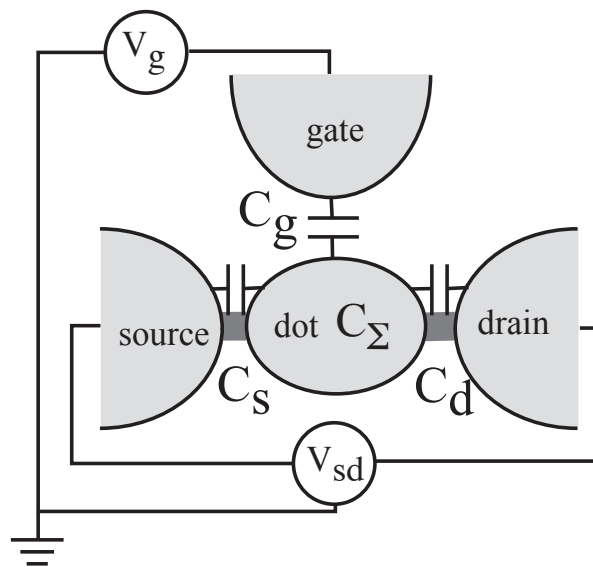


Figure 1: Schematic drawing of a typical electrode arrangement for a single electron transistor. The island has index 0, the source has index 1, the drain index 2 and the gate index 3. The elements of the capacitance matrix  $C_{ij}$  are numbered accordingly.

---

<sup>1</sup>Text adapted from Ref.[1]

## Single electron charging

The device which we want to consider is a so-called *single electron transistor* [ Fig. 1(a)] where a small island with the self-capacitance  $C_\Sigma$  is weakly coupled to source and drain contacts via tunnel barriers. At low enough temperatures and small bias voltage, the energy cost to add an extra electron onto the island may exceed the thermal energy ( $k_B T \ll e^2/C_\Sigma$ ) and the current through the island is blocked. This is the Coulomb blockade effect.

It was first suggested in the early 50's by Gorter [2] as an explanation for the observation [3, 4] of an anomalous increase of the resistance of thin granular metallic films with a reduction in temperature. More than 30 years later Fulton and Dolan [5] observed Coulomb blockade effects in a microfabricated metallic sample and initiated a huge number of experimental and theoretical studies. Today there are many text books and reviews [6, 7, 8, 9] on single electron systems both in metals and in semiconductor systems.

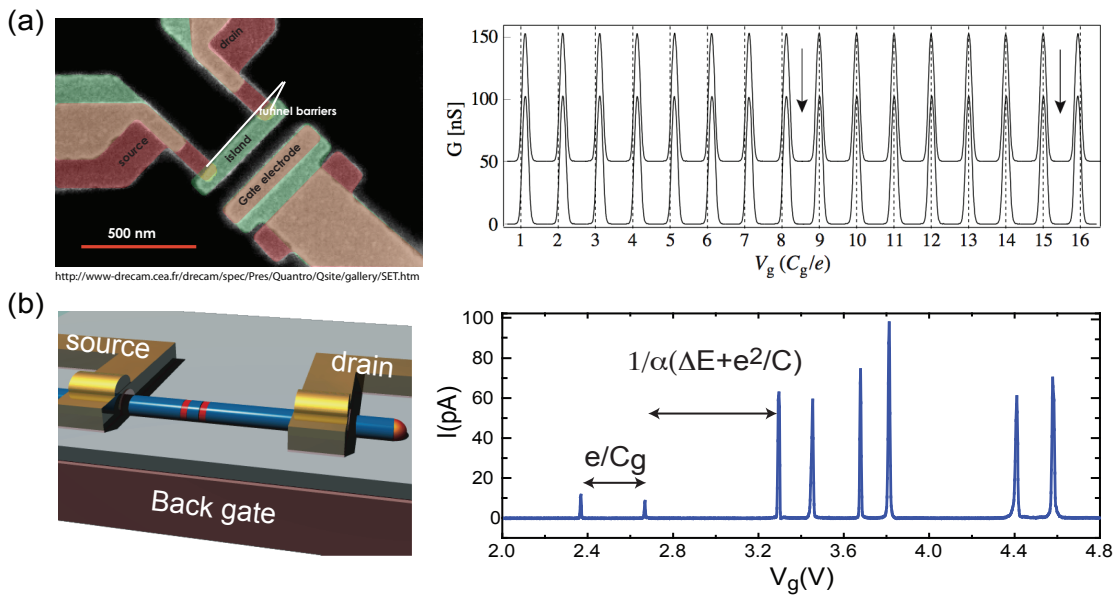


Figure 2: (a) Single electron transistor fabricated using shadow evaporation techniques. The metallic island is connected to source and drain contacts through two oxide tunnel barriers. (yellow). On the peak the number of electrons can fluctuate between  $N$  and  $N+1$ , in between transport is blocked due to the *Coulomb blockade* effect. Coulomb oscillations through a metallic device are periodic and show conductance peaks with identical heights (b) Nanowire quantum dot connected to source and drain. Coulomb peaks show different heights and are irregularly spaced.

---

## Coulomb blockade in metallic islands

We start with the situation shown in Fig. 1 where a small metallic particle(dot) is surrounded by a number of electrodes connected to voltage sources. As discussed in the lecture the charge state of such an arrangement can be described using a capacitance matrix which relates the induced charge on each of the electrodes to the potential change  $V_j$ .

$$\tilde{Q}_i = \sum_{j=0}^n C_{ij} V_j \quad (1)$$

Here,  $C_{ij}$  are the elements of the capacitance matrix describing the arrangement of conductors and  $\tilde{Q}_i$  denotes the charge that is induced on the island by the electrostatic potentials  $V_j$  on the gates and in the source and drain contacts. We will denote the dot with index 0, the source and drain contacts with index 1 and 2 respectively and the gate with index 3. Generally there will be more than one gate electrode (index 4 ... ) which will make the capacitance matrix of the system larger.

The electrostatic potential of the isolated dot in the presence of the gates is then given by

$$V_0(Q_0) = \frac{1}{C_\Sigma} \left( \underbrace{Q_0 - Q_{bg}}_{\tilde{Q}_0} - \sum_{j=1}^n C_{0j} V_j \right) \quad (2)$$

In typical Coulomb blockade experiments the bias voltage ( $V_{SD}$ ) is much smaller than the gate voltages and if we choose the electrostatic zero-point to be equal to the electro-chemical potential at source ( $j = 1$ ) and drain ( $j = 2$ ) we can identify the voltage applied to the gates with  $V_j$  in the above equation.  $Q_{bg}$  is the charge that remains on the dot (index 0) if all potentials are put to zero. This can vary from device to device e.g. because of the doping in the region of the dot. Due to overall charge neutrality the  $C_{ij}$  obey the relation  $\sum_{i=0}^n C_{ij} = 0$  and the self capacitance of the island is therefore given by  $C_\Sigma := C_{00} = -\sum_{j=1}^n C_{0j}$ . If the electron charge  $Q_0 = -eN$  on the island is quantized, the total electrostatic energy needed to charge the dot with  $N$  electrons at fixed  $V_j$  is

$$U(N) = \int_0^{-eN} V_0(Q_0) dQ_0 = \frac{e^2 N^2}{2C_\Sigma} + eN \left( \frac{Q_{bg}}{C_\Sigma} + \sum_{j=1}^n \frac{C_{0j}}{C_\Sigma} V_j \right) \quad (3)$$

Here, the external gates induce the displacement charge  $\sum_{j=1}^n \frac{C_{0j}}{C_\Sigma} V_j$ , which can be varied continuously by changing the gate voltages. (In electrostatics this is often referred to as the charging energy, which makes things confusing when talking about quantum dots!) From this we can now calculate the energy needed to charge the island with an additional electron assuming that there are already  $N$  electrons on the island

$$\tilde{\mu}_{N+1} = U(N+1) - U(N) = \frac{e^2}{C_\Sigma} \left[ N + \frac{1}{2} \right] + e \left( \frac{Q_{bg}}{C_\Sigma} + \sum_{j=1}^n \frac{C_{0j}}{C_\Sigma} V_j \right) \quad (4)$$

---

This difference between the total energies for  $N+1$  and  $N$  electrons is often referred to as the addition energy and will lead to the chemical potential as discussed below (sometimes, however, this is also called the charging energy). Here we put a  $\tilde{\mu}$  in order to denote that this is the difference between the electrostatic energies only, not including the single particle energies.  $\tilde{\mu}_{N+1}$  increases linearly with the number of electrons on the dot if the gate voltages are kept constant. By tuning the gates it is possible to tune  $\tilde{\mu}_{N+1}$  to lie between the electrochemical potentials in source and drain, allowing electrons to tunnel on and off the dot one at a time. A continuous change of the gate voltage then leads to the typical Coulomb blockade oscillations in the conductance through the dot as shown in Fig. 2(a). On a conductance peak the number of electrons can fluctuate between  $N$  and  $N+1$  while in the blockade region between two peaks the charge on the island is fixed. Being able to tune a current of sequential single electron tunneling by a gate voltage gave this device the name *single electron transistor*. In these considerations we have used only classical arguments to describe the properties of such a device. This is called the classical Coulomb blockade regime and it is a good description for metallic systems with a continuous density of states.

## Coulomb blockade in semiconductor quantum dots

We have mentioned before that the Fermi wavelength in semiconductor heterostructures is much larger than in metallic systems, due to the relatively small electron density in semiconductors. This means that in semiconductor nanostructures size quantization as well as Coulomb blockade effects will be important. The simplest model which combines both the Coulomb blockade effect and the energy spectrum of a quantum dot is the constant-interaction model [10].

### Constant interaction model

In the constant interaction model it is assumed that the total energy of the island is given by the sum of its single-particle energies plus the electrostatic energy  $U(N)$ :

$$E(N) = \sum_{i=1}^N \epsilon_i + U(N) = \sum_{i=1}^N \epsilon_i + \frac{e^2 N^2}{2C_\Sigma} + eN \left( \frac{Q_{bg}}{C_\Sigma} + \sum_{j=1}^n \frac{C_{0j}}{C_\Sigma} V_j \right) \quad (5)$$

Since the electrochemical potential is defined as the energy required to add the  $N$ th electron to a conductor, we can write  $\mu_N$  for a dot as

$$\mu_N = E(N) - E(N-1) = \epsilon_N + \frac{e^2}{C_\Sigma} \left( N - \frac{1}{2} \right) + e \left( \frac{Q_{bg}}{C_\Sigma} + \sum_{j=1}^n \frac{C_{0j}}{C_\Sigma} V_j \right). \quad (6)$$

The lever arm  $\alpha_i$  of gate  $i$  on the dot is defined by the ratio

$$\alpha_i := -\frac{C_{0i}}{C_\Sigma} \quad (7)$$

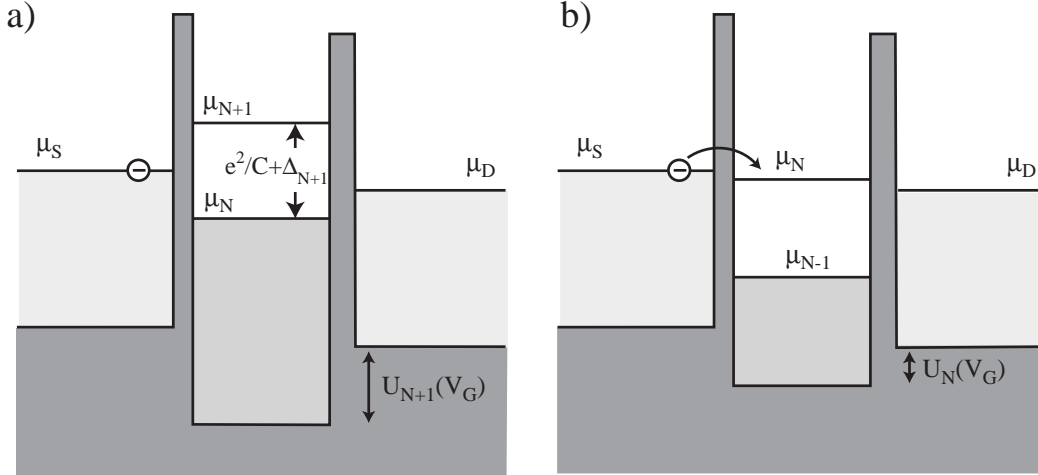


Figure 3: Energy diagram for a quantum dot. The two tunnel barriers connect the dot to the source and drain contacts. (a) Here, transport is blocked and the dot contains a fixed number of  $N$  electrons. (b) The gate voltage was tuned in order to align the chemical potential in the dot with that of source and drain. In this situation the number of electrons on the dot can fluctuate between  $N-1$  and  $N$  giving rise to a peak in the conductance.

The value of  $\alpha_i$  is always positive and in an experiment it typically varies with large changes in gate voltage. For metallic gates this nonlinearity is small and the leverarm is well defined. However in quantum dots where regions of a 2DEG are used as so-called in-plane gates the lever arm might change slowly as a function of the voltage applied to the gate making the relation between the chemical potential on the dot and gate voltage non-linear.

Transport through a quantum dot system can now be viewed in terms of the energy diagram of a double tunnel barrier arrangement like the one schematically depicted in Fig.3. Here, we first consider the situation at very small bias and low temperatures ( $eV_{bias}, k_B T \ll e^2/C_\Sigma$ ). In Fig. 3(a) transport through the dot is blocked due to the Coulomb blockade effect, with  $N$  electrons on the dot. By decreasing the gate voltage, the chemical potential  $\mu_N$  inside the dot [equation (6)] is raised until it aligns with that of the drain contact ( $\mu_D = \mu_N$ ) and an electron can leave the dot. If at the same time  $\mu_S \gtrsim \mu_D$  a current can flow and the number of electrons on the dot will fluctuate between  $N$  and  $N-1$ . When the gate voltage further decreases and  $\mu_S < \mu_N$  the dot is left with one electron less ( $N-1$ ) and the current is again blocked.

For a small bias we therefore have a peak in the conductance whenever  $\mu_N \approx \mu_S \approx \mu_D$ . If this is used to solve equation (6) for the gate voltage we find that the position of the peak maximum is given by

$$V_G^{(N)} = \frac{1}{e\alpha_G} \left[ \epsilon_N + \frac{e^2}{C_\Sigma} \left( N - \frac{1}{2} \right) - e \sum_{j=4}^n \alpha_j V_j + \frac{eQ_{bg}}{C_\Sigma} - \mu_S \right]. \quad (8)$$

---

## Addition spectroscopy

In the constant interaction model the evolution of the peak position as a function of an external parameter  $B$  such as the magnetic field has a very simple interpretation. Under the assumption that the capacitance coefficients  $C_{ij}$  and the background charge stay constant, the peak maximum position  $V_G^{(N)}$  [equation (8)] is a measure of the change of the corresponding single-particle level  $\epsilon_N(B)$  as a function of an external parameter such as the magnetic field. The separation between two peaks is given by

$$e\Delta V_G^{(N)} = \frac{1}{\alpha_G} (\mu_N - \mu_{N-1}) = \frac{1}{\alpha_G} \left( \underbrace{(\epsilon_N - \epsilon_{N-1})}_{\Delta_N} + \frac{e^2}{C_\Sigma} \right) \quad (9)$$

where  $\Delta_N$  is the single-particle level spacing. The influence of the space quantization can be nicely seen when we look at a measurement of a semiconducting nanowire quantum dot in Fig. 2(b). In contrast to Fig. 2(a) the Coulomb blockade peaks are unequally spaced and have various amplitudes. By subtracting  $1/\alpha_G(e^2/C_\Sigma)$  from each peak spacing it is therefore possible to reconstruct the single-particle spectrum of the dot. This method was first used in an experiment by McEuen [11] to reconstruct the energy spectrum of a dot in the quantum Hall effect regime.

In order to analyze a spectrum in a quantitative way it is necessary to know the value of the lever arm of the gate which is tuned. The easiest way to determine the lever arm is by measuring the Coulomb blockade diamonds, namely current-voltage characteristics through the dot as a function of the gate voltage.

## Charge stability diagrams and Coulomb diamonds

To this end we consider the same situation as above but for finite bias voltage  $V_{bias}$ . We assume that the bias is applied symmetrically to the source and drain contacts, which means  $\mu_S = \mu_0 + eV_{bias}/2$  and  $\mu_D = \mu_0 - eV_{bias}/2$  where  $\mu_0$  is the electrochemical potential in both contacts without an additional bias voltage. This now leads to a set of requirements for the situation where a configuration with  $N$  electrons on the dot is stable. For  $V_{bias} > 0$  one finds:

$$\begin{aligned} \mu_N &< \mu_0 - eV_{bias}/2 \\ \mu_{N+1} &> \mu_0 + eV_{bias}/2 \end{aligned}$$

for  $V_{bias} < 0$ :

$$\begin{aligned} \mu_N &< \mu_0 + eV_{bias}/2 \\ \mu_{N+1} &> \mu_0 - eV_{bias}/2 \end{aligned}$$

These inequalities can be translated into what we will call *borderline-equations* describing the line where the Coulomb blockade is lifted at the edge of the diamond

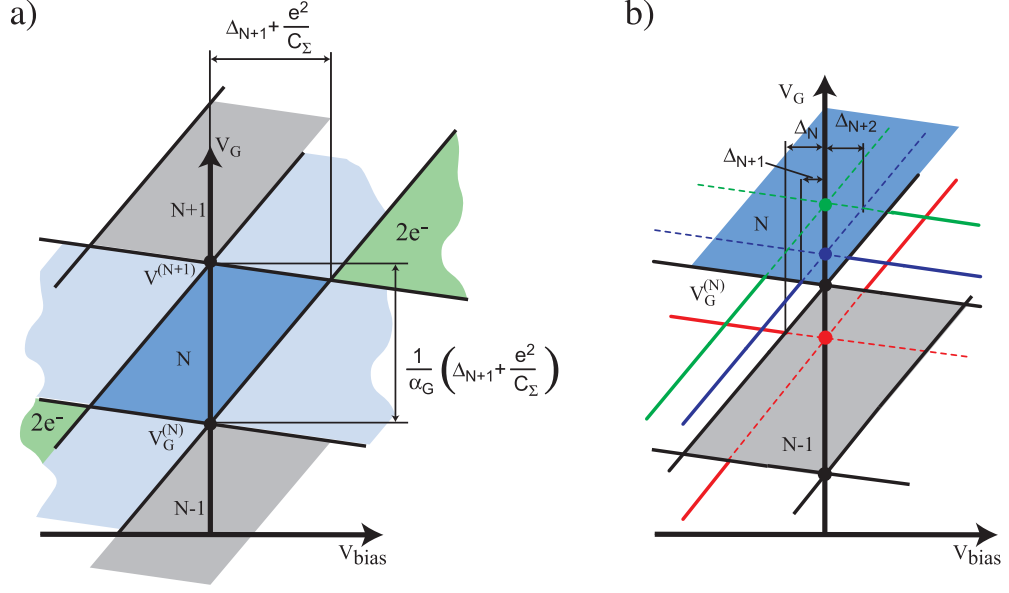


Figure 4: Coulomb blockade diamonds. (a) The current is blocked in the diamond shaped areas shaded in grey and dark blue. In these areas the number of electrons in the dot,  $N$ , is constant. Conductance peaks occur on the  $V_G$ -axis at points where neighboring diamonds touch (black dots). (b) Excited states move as lines parallel to the borderlines of the diamonds in the regions where the current is not blocked.

shaped region. Using the relation (6) we find for  $V_{bias} > 0$

$$V_G = \frac{1}{e\alpha_G} \left[ \epsilon_N + E_c \left( N - \frac{1}{2} \right) - \mu_0 + e(1 - \alpha_S + \alpha_D)V_{bias}/2 - e \sum_{j=4}^n \alpha_j V_j + \frac{eQ_{bg}}{C_\Sigma} \right]$$

$$V_G = \frac{1}{e\alpha_G} \left[ \epsilon_{N+1} + E_c \left( N + \frac{1}{2} \right) - \mu_0 - e(1 + \alpha_S - \alpha_D)V_{bias}/2 - e \sum_{j=4}^n \alpha_j V_j + \frac{eQ_{bg}}{C_\Sigma} \right]$$

Here,  $\alpha_S, \alpha_D$  are the lever arms of the source and drain contacts. If the dot is symmetric, e.g the tunnel barriers have the same geometry, then  $\alpha_S = \alpha_D$  and the borderlines have exactly the opposite slope  $\pm 1/(2\alpha_G)$ . The two lines cross at  $eV_{bias} = \Delta_{N+1} + e^2/C_\Sigma$ . Therefore, comparing the extent of the diamonds for positive bias with the separation of the corresponding Coulomb peaks gives a measure of the lever arm. Furthermore it turns out that the difference of the slopes of the two border lines is  $1/\alpha_G$  irrespective of the lever arms of source and drain. The situation is shown in detail in Fig. 4(a). In the central diamond (dark blue region) the probability of finding  $N$  electrons on the quantum dot is unity and the dot is in a stable  $N$ -electron configuration. The light blue diamonds extending from the Coulomb peaks (black dots) denote the regions where the probability for finding  $N$

electrons on the dot is between 0 and 1 and the electron number can fluctuate by one. Further away from the gate axis (green areas), the large bias ( $eV_{bias} > e^2/C_\Sigma$ ) allows for two electrons to tunnel at the same time. In a measurement of the differential conductance ( $\partial I/\partial V$ ) as a function of DC-bias  $V_{bias}$  and gate voltage the border lines will show up as peaks since this is where the current through the dot changes and a new transport channel opens/closes (cf. Fig. 5).

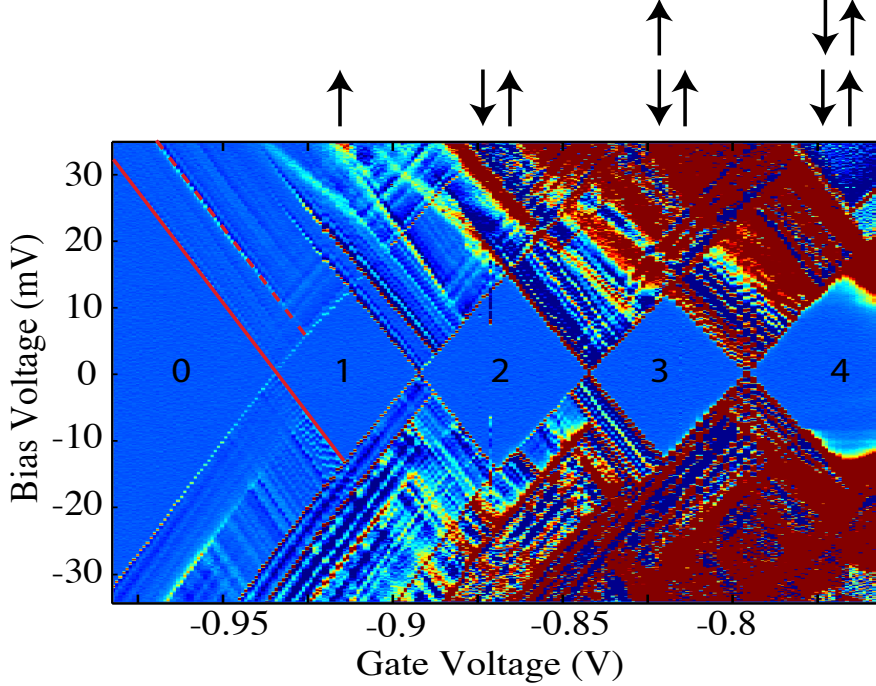


Figure 5: Measurement of Coulomb blockade diamonds in the differential conductance through a quantum dot. Blue(red) indicate regions of low(high) differential conductance  $\partial I/\partial V_{bias}$  respectively. The second diamond is a bit larger than it's neighboring ones indicating that the next orbital level is being occupied. The arrows at the top of the figure show how the levels are being filled with spins.

### Excited states

In the above discussion we have assumed that only a single level  $\epsilon_N$  contributes to the transport through the dot. This is not true if  $eV_{bias} > \Delta_{N+1}$ . Here  $\Delta_{N+1}$  is the energy difference between the  $N + 1$  electron ground state and it's first excited state. Within the constant interaction picture this is equivalent to the  $N + 1$ st single particle energy spacing  $\Delta_{N+1} = \epsilon_{N+1} - \epsilon_N$ . Therefore, additional single-particle levels become accessible within the bounds given by the bias voltage and lead to an increase of the current through the dot and to additional boundary lines in the differential conductance. This is shown in Fig. 4(b) where for each Coulomb peak additional lines occur outside the blockade diamonds. For all the

---

elastic processes (energy conserving regarding the dot energy) the border lines for each Coulomb blockade peak are simply shifted by the single-particle level spacings  $1/\alpha_G\Delta$ . (indicated by the bold dots on the gate axis. In  $V_{bias}$  direction the line of the ground state and that of the excited state are separated by  $2 * \Delta$  in analogy to the separation of the two tips of a Coulomb diamonds.) In real dots with many electrons there are also more complex collective excitations [12] that have to be considered. In addition, not all processes have the same amplitude, which means that some of the lines in the diamonds are suppressed. This can be seen in Fig. 5 where the measurement of such diamonds in a quantum dot is shown. The differential conductance is plotted on a logarithmic colorscale in order to bring out the excited states more clearly.

## Amplitude and line shape of the conductance peaks

Up to this point we have treated the dot as an isolated system at zero temperature. In a real system the dot is connected to source and drain. If we continue in the language of the single-particle picture then each level  $i$  will have a slightly different coupling  $\Gamma_i^S, \Gamma_i^D$  due to the different overlap of its wavefunction with source and drain contacts. It follows that the corresponding level has a finite width given by  $\hbar\Gamma_i = \hbar\Gamma_i^S + \hbar\Gamma_i^D$ . This average inverse lifetime is used to discriminate two limiting regimes in theory, namely the weak coupling limit  $\hbar\Gamma \ll k_B T$  and the strong coupling regime  $k_B T \lesssim \hbar\Gamma$ .

### Weak-coupling regime

A model for this regime at finite temperatures, was first discussed in 1991 by Beenakker [10]. Here, the energy levels in the dot are treated as delta functions in the density of states inside the dot ( $\hbar\Gamma \ll k_B T$ ). Here, we only give the limiting form which is important for most measurements taken in the weak coupling limit, namely the conductance in the *quantum-Coulomb blockade* regime ( $\hbar\Gamma \ll k_B T \ll \Delta, e^2/C_\Sigma$ ). *A single level then contributes to the current on a Coulomb peak* and the conductance is given by

$$G^{(i)} = \frac{e^2}{4k_B T} \left( \frac{1}{\Gamma_i^S} + \frac{1}{\Gamma_i^D} \right)^{-1} \cosh^{-2} \left( \frac{\alpha_G (V_G^{(i)} - V_G)}{2k_B T} \right) \quad (10)$$

Here,  $V_G^{(i)}$  is the position of the  $i$ 'th Coulomb peak on the gate voltage axis. With increasing temperature the amplitude of the peak decays with  $1/T$ . Apart from the temperature dependence, the peak amplitude also reflects the coupling to source and drain given by the series resistance of the two barriers for level  $\epsilon_i$ . A clear signature of this regime is therefore the uncorrelated variation of the Coulomb peak height as the gate voltage is tuned. Note, that we have neglected spin in this consideration. In the simplest case if we assume degenerate spin levels the peak amplitude would

lead to peak pairs with similar amplitudes since the same orbital level is charged with spin up and spin down.

**for the interested reader** - When the temperature smearing of the Fermi-function in source and drain becomes comparable to a neighboring single-particle level spacing, the additional channel can lead to an anomalous increase of the conductance maximum with temperature. Such a situation is shown in Fig. 6. Three levels are considered where the middle level (2) and the uppermost level (3) are quite close ( $\Delta = 20meV$ ). The lever arm of the gate is assumed to be unity and the coupling of the three levels is chosen as indicated in Fig. 6(a) where the middle level has the weakest coupling. Here, the amplitude of the central peak first increases with temperature when level 3 starts to contribute to the current, then the current drops as expected. A similar behavior is expected for an increase in the bias voltage. The central peak will increase in amplitude once the excited state with strong coupling is energetically accessible. This is shown in Fig. 6(c). The conductance is small at  $V_{bias} = 0$  and suddenly increases for  $eV_{bias} > \Delta_3$ . The opposite is true for peak 3. Once the first excited state gets a finite occupation probability the current suddenly drops. This leads to strips of negative differential conductance (NDC) where the current drops as the bias is increased (red regions marked by arrows). Qualitatively the long lifetime of the excited state blocks the sequential tunneling current through the resonant channel due to the Coulomb blockade which permits only one additional electron on the dot. Figure 6(d) shows the case where the coupling of the middle level is made asymmetric with respect to source and drain. This leads to asymmetries in the diamonds and in some cases may lead to the complete suppression of one of the borderlines. In real dots it is quite difficult to make the barriers exactly the same. Apart from these orbital effects states with a large groundstate spin will lead to similar features in a phenomenon called spin blockade [13].

In all of these cases the peak shape stays roughly the same, except for a slight increase of the width. This means that the FWHM (full width half maximum) of a peak can be used as an upper bound for the electron temperature:

$$T \leq \frac{e\alpha_G\Delta V_G^{FWHM}}{4\text{acosh}(\sqrt{2})k_B} \approx 3.29K/mV\alpha_G\Delta V_G^{FWHM} \quad (11)$$

Here,  $\alpha_G\Delta V_G^{FWHM}$  is the width of the Coulomb peak in units of the dot energy.

In the case where many levels contribute to each Coulomb peak, namely where  $\hbar\Gamma, \Delta \ll k_B T \ll e^2/C_\Sigma$  the peaks all have the same height given by the series addition of the resistance of the two barriers

$$\left( \frac{1}{\Gamma^S} + \frac{1}{\Gamma^D} \right)^{-1}$$

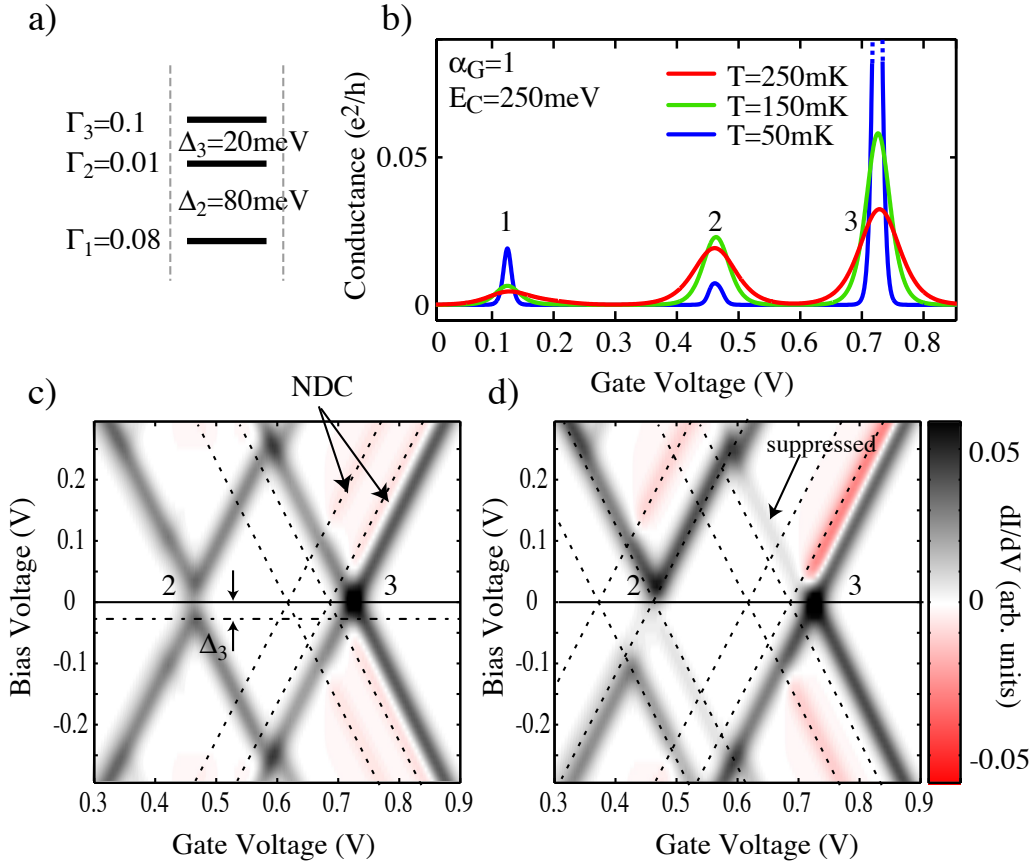


Figure 6: Calculations of peaks and diamonds in the model by Beenakker. (a) Three single-particle levels are considered with different coupling and separation  $\Delta$ . (b) Peak-shapes at different temperatures. The central peak shows an anomalous temperature behavior. (c) Differential conductance through the dot as a function of both gate and bias voltage. When the excited states are accessible due to a finite bias they can strongly modify the current and even lead to regions of negative differential conductance (NDC). (d) Asymmetric coupling  $\Gamma_2^D > \Gamma_2^S$ . Some of the borderlines of the diamonds are completely suppressed.

---

This is called the *classical Coulomb blockade* regime since size quantization is no longer relevant (e.g. in metallic SET's). The peak shape is very similar to the quantum limit except that the width is larger by a factor of 5/4.

### Strong-coupling regime

The strong coupling limit ( $k_B T \lesssim \hbar \Gamma$ ) cannot be treated in the formalism discussed above. The case of noninteracting electrons ( $e^2/C_\Sigma \ll k_B T, \hbar \Gamma, \Delta$ ) is closely related to the problem of resonant transmission through a double barrier [14, 15] as we have discussed it in the lecture. The line-shape of a single resonant level is simply a Lorentzian and its conductance is given by the well known Breit-Wigner formula [16]

$$G = \frac{2e^2}{h} \left( \frac{1}{\Gamma^S} + \frac{1}{\Gamma^D} \right)^{-1} \frac{\hbar^2 \Gamma}{\alpha_G^2 (V_G^{max} - V_G)^2 + (\hbar \Gamma / 2)^2} \quad (12)$$

Here,  $\Gamma = \Gamma^S + \Gamma^D$  is assumed to be independent on the level index  $i$  and the factor 2 is for spin degeneracy. Since charge effects are neglected, the tunneling no longer needs to be sequential (=one electron at a time) and the two channels for each spin direction add up. In this limit higher order processes are important [9] and in the case of  $\hbar \Gamma > \Delta$  inelastic transitions in the dot reduce the conductance and broaden the resonant level [14, 15].

### Transmission phase of a quantum dot

Recently several experiments have investigated the transmission phase of a quantum dot embedded in one of the arms of an Aharonov Bohm (AB)-ring [17, 18, 19, 20]. The basic idea was to extract the phase of the transmission through the quantum dot from the phase shift of the AB-oscillations in the conductance through the ring as a function of magnetic field. In order to explain a phase shift of  $\pi$ , the complex transmission amplitude of a Breit-Wigner resonance was used [18](see problem 5.12 in the book by Davies)

$$t_{QD} = iC_N \frac{\Gamma_N/2}{E_F - E_N + i\Gamma_N/2}. \quad (13)$$

Here,  $C_N$  is a complex amplitude,  $E_F$  the energy of the electrons transmitted through the device and  $E_N$  and  $\Gamma_N$  the energy and width of the resonance in the quantum dot. The resulting behavior of the phase and amplitude of  $t_{QD}(E_F - E_N)$  are shown in Fig. 7 for  $C_N = 1$  and  $\Gamma_N = 20$ .

### In-plane magnetic field

In a magnetic field parallel to the plane of the quantum dot (for a semiconducting nanowire perpendicular to the wire, for a dot in a 2DEG parallel to the surface) the

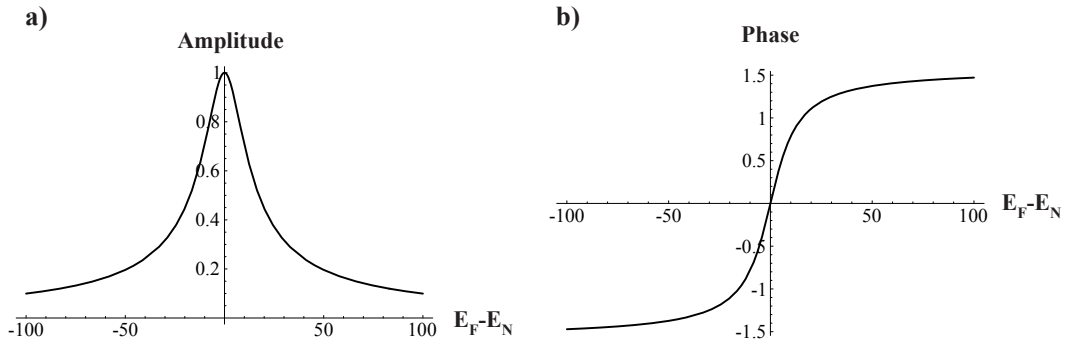


Figure 7: Amplitude  $|t_{QD}|$ (a) and phase  $\arg t_{QD}$ (b) of the transmission  $t_{QD}(E_F - E_N)$  through a quantum dot as calculated using a Breit-Wigner Ansatz for the conductance resonance line shape.

chemical potential of the dot has two additional terms

$$\mu_N = \epsilon_N + (N + \frac{1}{2}) \frac{e^2}{C_\Sigma} - \gamma_N B_{\parallel}^2 + (s_z^{(N)} - s_z^{(N-1)}) g^* \mu_B B_{\parallel} \quad (14)$$

One is called the diamagnetic shift which is parabolic in  $B_{\parallel}$  and describes the shift of the energy levels due to a squeezing of the wavefunctions in strong magnetic fields. The other term is the Zeeman splitting which is linear in B. Here, we restrict ourselves to a short discussion of the Zeeman term since other magnetic field effects, namely on the spectrum of a harmonic oscillator potential, are treated in the book.

### Zeeman splitting

So far we have neglected spin-effects altogether in our considerations. In the zero magnetic field case this means that we have simply assumed degenerate spin states or in other words the filling of each orbital level first with a spin up and then a spin down electron. Within the constant interaction picture this leads to a sequence of *spin pairs* namely Coulomb peaks which are separated only by the interaction energy  $1/\alpha_G e^2/C_\Sigma$ . In this case the groundstate spin of the dot switches between  $s_z = 0$  for an even number of electrons and  $s_z = \pm 1/2$  for odd N. Since the addition energy results from the difference  $\mu_N = E(N) - E(N - 1)$  the Coulomb peaks will be shifted proportional to

$$\Delta E_{zeeman} = (s_z^{(N)} - s_z^{(N-1)}) g^* \mu_B B_{\parallel} = \pm \frac{1}{2} g^* \mu_B B_{\parallel} \quad (15)$$

here  $s_z^N$  is the ground state spin for N electrons on the dot and  $g^*$  is the effective g-factor for the electrons in the dot.

In these considerations we have assumed that the lever arm  $\alpha_G$  is independent of the magnetic field. In addition, the diamagnetic shift of both the contacts as well as the dot will obscure this picture of a linear Zeeman splitting. A possible solution to

---

this is found by the assumption that both  $\alpha_G$  and  $\gamma_N$  are slowly varying functions of the gate voltage which means that more reliable information can be obtained from differences of neighboring peak positions. Here, we have only discussed the simplest case of including spin in the constant interaction picture. In a system where exchange effects are important (e.g. orbital filling according to Hunds rules.) this picture breaks down.

# Bibliography

- [1] A. Fuhrer, Ph.D. thesis, Swiss Federal Institute of Technology (2003).
- [2] C. J. Gorter, *Physica* **17**, 777 (1951).
- [3] R. Lambeir, A. Vanitterbeek, and G. J. Vandenberg, *Physica* **16**, 907 (1950).
- [4] N. Mostovetch and B. Vodar, *Compt,Rend* **230**, 934 (1950).
- [5] T. A. Fulton and G. J. Dolan, *Phys. Rev:lett.* **59**, 109 (1987).
- [6] P. Hawrylak, L. Jacak, and A. Wojs, *Quantum dots* (Springer Verlag, Berlin, 1998).
- [7] H. Grabert and M. H. Devoret, *Single Charge Tunneling* (Plenum Press, New York, 1992).
- [8] T. Ando, Y. Arakawa, K. Furuya, S. Komiyama, and H. Nakashima, eds., *Mesoscopic Physics and Electronics* (Springer, 1998).
- [9] L. P. Kouwenhoven, C. M. Marcus, P. L. McEuen, S. Tarucha, R. M. Westervelt, and N. S. Wingreen, in *Nato ASI conference proceedings*, edited by L. P. Kouwenhoven, G. Schön, and L. L. Sohn (Kluwer, Dordrecht, 1997), pp. 105–214.
- [10] C. W. J. Beenakker, *Phys. Rev. B* **44**, 1646 (1991).
- [11] P. L. McEuen, E. B. Foxman, U. Meirav, M. A. Kastner, Y. Meir, N. S. Wingreen, and S. J. Wind, *Phys. Rev. Lett.* **66**, 1926 (1991).
- [12] D. Pfannkuche and S. Ulloa, *Phys. Rev. Lett* **74**, 1194 (1995).
- [13] D. Weinmann, W. Häusler, and B. Kramer, *Phys. Rev. Lett.* **74**, 984 (1995).
- [14] M. Büttiker, *Phys. Rev. B.* **33**, 3020 (1986).
- [15] A. D. Stone and P. A. Lee, *Phys. Rev. Lett.* **54**, 1196 (1985).
- [16] G. Breit and E. Wigner, *Phys. Rev.* **49**, 519 (1936).

- [17] A. Yacoby, M. Heiblum, D. Mahalu, and H. Shtrikman, *Phys. Rev. Lett.* **74**, 4047 (1995).
- [18] R. Schuster, E. Buks, M. Heiblum, D. Mahalu, and V. U. H. Shtrikman, *Nature* **385**, 417 (1997).
- [19] Y. Ji, M. Heiblum, and H. Shtrikman, *Phys. Rev. Lett.* **88**, 076601 (2002).
- [20] K. Kobayashi, H. Aikawa, S. Katsumoto, and Y. Iye, *Phys. Rev. Lett* **88**, 256806 (2002).
- [21] Y. M. Blanter, A. D. Mirlin, and B. A. Muzykantskii, *Phys. Rev. Lett.* **78**, 2449 (1997).
- [22] H. U. Baranger, D. Ullmo, and L. I. Glazman, *Phys. Rev. B* **61**, R2425 (2000).
- [23] P. W. Brouwer, Y. Oreg, and B. I. Halperin, *Phys. Rev. B* **60**, R13977 (1999).
- [24] H. Jiang, H. U. Baranger, and W. Yang, *Phys. Rev. Lett.* **90**, 026806 (2003).
- [25] W. J. D. Haas, J. D. Boer, and G. J. van der Berg, *Physica* **1**, 1115 (1933).
- [26] J. Kondo, *Progr. Theor. Phys.* **37**, 37 (1964).
- [27] L. I. Glazman and M. E. Rai, *JETP Lett.* **47**, 452 (1988).
- [28] T. K. Ng and P. A. Lee, *Phys. Rev. Lett* **61**, 1768 (1988).
- [29] D. Goldhaber-Gordon, H. Shtrikman, D. Mahalu, D. Abusch-Magder, U. Meirav, and M. A. Kastner, *Nature* **391**, 156 (1998).
- [30] F. D. M. Haldane, *Phys. Rev. Lett* **40**, 416 (1978).
- [31] S. M. Cronenwett, T. H. Oosterkamp, and L. P. Kouwenhoven, *Science* **281**, 540 (1998).
- [32] J. Schmid, J. Weis, K. Eberll, and K. v. Klitzing, *Physica B* **256**, 182 (1998).
- [33] H. Jeong, A. M. Chang, and M. R. Melloch, *Science* **293**, 2221 (2001).
- [34] J. Nygard, D. H. Cobden, and P. E. Lindelof, *Nature* **408**, 342 (2000).
- [35] W. Liang, M. P. Shores, M. Bockrath, J. R. Long, and H. Park, *Nature* **417**, 725 (2002).
- [36] U. F. Keyser, C. Fuhner, S. Borck, R. J. Haug, M. Bichler, G. Abstreiter, and W. Wegscheider (2002), *cond-mat/0206262*.